Check for updates

IET Control Theory & Applications

WILEY

IET The Institution of Engineering and Technology

ORIGINAL RESEARCH OPEN ACCESS

Enhanced Hiking Optimization Algorithm for Robust PID Control in Doubly-Fed Induction Generator Systems for Wind Energy Applications

Davut Izci[1,2] | Fatma Artun[3] | Serdar Ekinci[4] | Mohit Bajaj[5,6] | Vojtech Blazek[7] | Ievgen Zaitsev[8]

[1]Department of Electrical and Electronics Engineering, Bursa Uludag University, Bursa, Turkey | [2]Applied Science Research Center, Applied Science Private University, Amman, Jordan | [3]Institute of Graduate Studies, Batman University, Batman, Turkey | [4]Department of Computer Engineering, Bitlis Eren University, Bitlis, Turkey | [5]Department of Electrical Engineering, Graphic Era (Deemed to Be University), Dehradun, India | [6]Graphic Era Hill University, Dehradun, India | [7]ENET Centre, CEET, VSB-Technical University of Ostrava, Ostrava, Czech Republic | [8]Department of Theoretical Electrical Engineering and Diagnostics of Electrical Equipment, Institute of Electrodynamics, National Academy of Sciences of Ukraine, Kyiv, Ukraine

Correspondence: Mohit Bajaj (mohitbajaj.ee@geu.ac.in) | Ievgen Zaitsev (zaitsev@i.ua)

Received: 25 March 2025 | **Revised:** 9 August 2025 | **Accepted:** 24 August 2025

Funding: This research is funded by European Union under the REFRESH—Research Excellence For Region Sustainability and High-Tech Industries Project via the Operational Programme Just Transition under Grant CZ.10.03.01/00/22_003/0000048; in part by the National Centre for Energy II and ExPEDite Project a Research and Innovation Action to Support the Implementation of the Climate Neutral and Smart Cities Mission Project TN02000025; and in part by ExPEDite through European Union's Horizon Mission Programme under Grant 101139527. The authors would like to express their sincere gratitude to Lukas Prokop and Stanislav Misak for their exceptional supervision, project administration, and overall guidance throughout the course of this project. Their expertise and support were instrumental to its success.

ABSTRACT

This paper addresses the critical control challenges inherent in doubly fed induction generator (DFIG) systems, which are pivotal components of modern wind energy conversion systems (WECS). These systems often face performance degradation due to their nonlinear dynamics, sensitivity to grid disturbances, and difficulty in achieving robust control under fluctuating operational conditions. To tackle these issues, this study proposes an innovative approach for optimizing proportional-integral-derivative (PID) controller parameters using the hiking optimization algorithm (HOA). Inspired by Tobler's walking function, HOA is integrated with an enhanced version of the Zwe-Lee Gaing (ZLG) objective function that incorporates penalty terms for overshoot, settling time, control effort, and abrupt signal variations. This enables a robust balance between transient and steady-state performance in dynamic environments. Extensive simulations validate the effectiveness of the HOA-optimized PID controller against five state-of-the-art met heuristic algorithms: starfish optimization algorithm, grey wolf optimizer (GWO), dragonfly algorithm (DA), flow direction algorithm (FDA), and sine-cosine algorithm (SCA). The results demonstrate that HOA achieves superior performance across all key metrics, including zero overshoot, rapid settling time (0.08922 s), and minimal steady-state error. Statistically, HOA maintains the highest reliability with a standard deviation of just 0.0013 over 30 independent trials. In the frequency domain, HOA outperforms competitors by achieving the highest phase margin (87.163) and gain margin (26.11 dB), ensuring robust stability. The proposed controller also excels in disturbance rejection and input tracking under varying conditions. These findings establish HOA

Abbreviations: ANN, artificial neural network; ASO, atom search optimization; BFO, bacterial foraging optimization; DA, dragonfly algorithm; DFIG, doubly-fed induction generator; FDA, flow direction algorithm; FOPID, fractional order PID controller; GSA, gravitational search algorithm; GWO, grey wolf optimizer; h-ASPSO, hybrid atom search and particle swarm optimization; HGS, hunger games search algorithm; HOA, hiking optimization algorithm; Imp-HGS, improved hunger games search algorithm; MPC, model predictive control; PI, proportional–integral controller; PID, proportional–integral–derivative; PSO, particle swarm optimization; RSA, reptile search algorithm; SCA, sine-cosine algorithm; SFOA, starfish optimization algorithm; WECS, wind energy conversion system; ZLG, Zwe-Lee Gaing's cost function.

This is an open access article under the terms of the Creative Commons Attribution License, which permits use, distribution and reproduction in any medium, provided the original work is properly cited.

© 2025 The Author(s). *IET Control Theory & Applications* published by John Wiley & Sons Ltd on behalf of The Institution of Engineering and Technology.

as a powerful and reliable optimization tool for advanced PID control of DFIG systems, with broader applicability in industrial control systems requiring high performance and adaptability.

1 | Introduction

The integration of renewable energy sources into modern power systems has significantly increased in recent years [1], driven by the global pursuit of sustainable and environmentally friendly energy solutions [2]. Among these sources, wind energy stands out due to its abundance and cost-effectiveness. The DFIG has emerged as a dominant technology in WECS because of its high efficiency, variable speed capability, and cost-effectiveness [3]. However, the inherent complexity of DFIG systems introduces challenges, including stability issues, sensitivity to grid disturbances, and the need for precise control to maintain performance [4].

1.1 | Control Architectures in DFIG-Based Systems

Various control strategies have been developed to address the dynamic behaviour and nonlinearities in DFIG-based WECS. Conventional PID controllers remain widely adopted due to their simplicity and ease of implementation in industrial applications [4], despite the growing trend toward more sophisticated variants. For instance, fractional-order PID (FOPID) controllers improve frequency-domain response by introducing additional tuning flexibility [5], while adaptive neuro-fuzzy inference systems enhance transient performance under varying wind conditions [6].

More recent studies have explored alternative structures such as sigmoid-PID [7], BELBIC-PID [8], PIDD^2 [9], and PIDA [10] controllers to further adapt to uncertainties and disturbances in WECS. Although these variants provide enhanced control performance, they often require complex modelling, higher computational loads, or extended tuning efforts, making them less suitable for scalable deployment. In this context, a well-tuned classical PID controller offers a robust and interpretable alternative, especially when optimized with intelligent algorithms that can unlock its full potential.

1.2 | Optimization Tools for Controller Tuning

Optimization techniques have become integral to the design and fine-tuning of control strategies for DFIG systems. Numerous metaheuristic approaches have been proposed to improve tuning accuracy and adaptability. For instance, the particle swarm optimizer has been integrated with model predictive control frameworks to minimize switching losses and harmonic distortions [11], while the thermal exchange optimizer has enhanced PI tuning for rotor and grid-side converters [12].

Other advanced tools include the ant lion optimizer for FOPI controllers [5], differential evolution for minimizing error metrics [13], hybrid approaches involving artificial neural networks with genetic-ant colony algorithms [14], and ecosystem-inspired optimizers for damping control in multimachine environments [15] Additionally, neuro-fuzzy DTC schemes and cascaded ANN controllers have demonstrated strong results in torque control and power quality enhancement [6, 16]. Despite the abundance of available algorithms, each has limitations in terms of convergence speed, solution diversity, or sensitivity to parameter settings. This underscores the importance of exploring novel optimizers that can deliver consistent and robust performance in high-dimensional, dynamic control problems.

1.3 | Proposed Approach and Justification

This study proposes the use of the HOA [17], a recent human-inspired metaheuristic, to optimize PID controller parameters for a DFIG-based wind energy system. HOA's design is based on Tobler's hiking behaviour [18] and employs elevation-based walking dynamics to guide the exploration of the solution space. The optimization process is guided by a modified ZLG objective function [19], which introduces penalty terms to simultaneously minimize overshoot, settling time, control effort, and abrupt changes in control signals. This tailored cost function enhances both transient and steady-state performance, ensuring controller robustness under fluctuating operational conditions.

The performance of the proposed methodology was evaluated through extensive simulations, focusing on statistical performance, time-domain response, frequency-domain analysis, and dynamic tests. The HOA was compared with five state-of-the-art metaheuristic algorithms: starfish optimization algorithm [20], GWO [21], DA [22], FDA [23], and SCA [24]. Statistical metrics such as mean, median, standard deviation and best and worst results were evaluated across 30 independent trials. The results revealed that HOA consistently outperformed its competitors, delivering minimal standard deviation and tightly clustered best and worst outcomes, indicating high reliability and robustness in PID controller optimization.

In time-domain performance analysis, HOA demonstrated superior transient behaviour by achieving zero overshoot, the fastest settling time, and no peak time, outperforming its counterparts in maintaining dynamic stability. Additionally, frequency-domain analysis using Bode plots highlighted HOA's enhanced phase and gain margins, signifying improved robustness and system stability. Dynamic performance tests further validated HOA's effectiveness in input signal tracking and external disturbance rejection, where it achieved precise tracking with negligible steady-state error and efficiently mitigated disturbances under varying operational conditions.

In addition to direct algorithmic comparisons, the study also references several optimization methods from existing literature,

17518652, 2025, 1, Downloaded from https://ietresearch.onlinelibrary.wiley.com/doi/10.1049/cth2.70071 by Bursa Uludag University Kutuphane ve Dokumantasyon, Wiley Online Library on [07/09/2026]. See the Terms and Conditions (https://onlinelibrary.wiley.com/terms-and-conditions) on Wiley Online Library for rules of use; OA articles are governed by the applicable Creative Commons License

including RSA [25], bacterial foraging optimization (BFO) [26], gravitational search algorithm (GSA) [26], particle swarm optimization (PSO) [26], atom search optimization (ASO) and its hybrid version with PSO [27], hunger games search algorithm and its improved version [28]. While these methods have shown varying degrees of success in similar contexts, the comparative results indicate significant advantages of HOA as it provides improved balance between exploration and exploitation and has demonstrated high reliability in global optimization tasks [17].

1.4 | Contributions and Organization

The key contributions of this work are outlined as follows:

- A PID controller structure is retained for its simplicity and industrial practicality, and its performance is enhanced through intelligent tuning.
- The HOA is introduced for the first time in DFIG-based control contexts to demonstrate its robustness and convergence quality.
- An improved ZLG objective function is employed to refine controller performance metrics comprehensively.
- The proposed approach is benchmarked against five well-established optimizers (SFOA, GWO, DA, FDA, and SCA) across 30 independent trials using statistical, time-domain, and frequency-domain evaluations.
- Extensive simulations confirm HOA's superior reliability, disturbance rejection, and adaptability compared to its counterparts.

The remainder of the paper is organized as follows. Section 2 presents the operational principles of DFIG systems. Section 3 details the structure of the proposed HOA. Section 4 introduces the objective function-driven HOA-based PID control scheme. Section 5 discusses the results and comparative analysis, and Section 6 concludes the paper with key findings and future directions.

2 | Modeling, Dynamics, and Control of Wind Energy Conversion via DFIG

2.1 | Energy Conversion in Wind Turbines

Wind turbines are devices used to convert kinetic wind energy into electrical energy. The power coefficient of wind turbines (C_p) depends on factors such as the blade pitch angle (β) and the blade tip speed ratio (TSR) (λ). This coefficient shows how efficiently the wind turbine converts its kinetic energy into electrical energy. According to the Betz limit, this power production cannot exceed 0.59, meaning that wind turbines can convert at most 59% of the energy in the wind into mechanical energy. The mechanical output power (P_w) obtained from wind turbines is given in Equation (1).

$$P_w = \frac{1}{2}\rho\pi R^2 V^3 C_p(\beta, \lambda) \tag{1}$$

This mechanical power is proportional to the cube of the wind speed, which depends on the wind density (ρ) and the wind speed (V). The C_p (β, λ) function is determined by observing the turbine blades' pitch angle and TSR and the turbine's characteristics. According to this equation, the turbine's production capacity varies depending on the wind speed and the aerodynamic properties of the blades. This explanation helps to optimize the turbine's production characteristics and understand the important features.

2.2 | Turbine Dynamics

In order for wind turbines to operate efficiently and reliably, the dynamic properties of the turbine must be well understood and modelled. The Equations (2)–(7) can be used as a model of the dynamic characteristics of the DFIG's stator and rotor voltages and fluxes in the d-q reference frame. These equations form an important basis for understanding and analysing the electromechanical behaviour of the system [29].

$$\begin{bmatrix} Vds \\ Vqs \end{bmatrix} = Rs \begin{bmatrix} Ids \\ Iqs \end{bmatrix} + \frac{d}{dt}\begin{bmatrix} \varphi ds \\ \varphi qs \end{bmatrix} + \omega_s \begin{bmatrix} 0 & -1 \\ 1 & 0 \end{bmatrix}\begin{bmatrix} \varphi ds \\ \varphi qs \end{bmatrix} \tag{2}$$

$$\begin{bmatrix} Vdr \\ Vqr \end{bmatrix} = Rr \begin{bmatrix} Idr \\ Iqr \end{bmatrix} + \frac{d}{dt}\begin{bmatrix} \varphi dr \\ \varphi qr \end{bmatrix} + s\omega_s \begin{bmatrix} 0 & -1 \\ 1 & 0 \end{bmatrix}\begin{bmatrix} \varphi dr \\ \varphi qr \end{bmatrix} \tag{3}$$

$$s\,(slip\ ratio) = \frac{\omega_s - \omega_r}{\omega_s} \tag{4}$$

$$\begin{bmatrix} \varphi ds \\ \varphi qs \\ \varphi dr \\ \varphi qr \end{bmatrix} = \begin{bmatrix} L_s & 0 & L_m & 0 \\ 0 & L_s & 0 & L_m \\ L_m & 0 & L_r & 0 \\ 0 & L_m & 0 & L_r \end{bmatrix}\begin{bmatrix} Ids \\ Iqs \\ Idr \\ Iqr \end{bmatrix} \tag{5}$$

$$L_s = L_{Is} + L_m \tag{6}$$

$$L_r = L_{Ir} + L_m \tag{7}$$

In these equations, Rs and Rr represent the resistances of the stator and rotor windings; leakage inductances are expressed as L_{Is} and L_{Ir}, and mutual inductances are expressed as L_m. V, I and φ in the d-q coordinates represent voltage, current and flux, respectively. The speeds generated by the stator and rotor currents are expressed by ω_s and ω_r, while the slip ratio of the machine is expressed by s [30].

In order to improve the control of the grid-connected DFIG system, a situation is considered where the stator flux is constant and the stator resistance Rs can be neglected. In this case $\varphi ds = \varphi s$ and $\varphi qs = 0$ are accepted. In this way, the equations related to the stator blocks and flux can be transformed into a simpler form as follows. Neglecting the stator resistance simplifies both the solution of the extended model and the system controls.

$$Vds = \frac{d\varphi ds}{dt} = 0 \tag{8}$$

$$V_{qs} = V_s = \omega_s\,\varphi ds \tag{9}$$

17518652, 2025, 1, Downloaded from https://ietresearch.onlinelibrary.wiley.com/doi/10.1049/cth2.70071 by Bursa Uludag University Kutuphane ve Dokumantasyon, Wiley Online Library on [07/09/2026]. See the Terms and Conditions (https://onlinelibrary.wiley.com/terms-and-conditions) on Wiley Online Library for rules of use; OA articles are governed by the applicable Creative Commons License

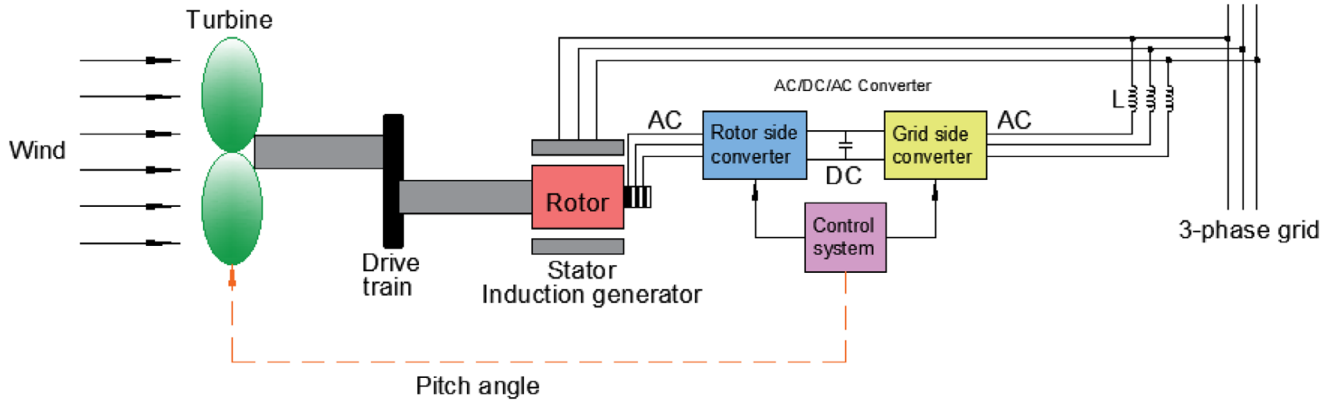


FIGURE 1 | DFIG and grid connection.

The active and reactive power of the stator can be shown by the following equations [31]:

$$P_s = -\frac{L_m}{L_s} V_s I_{qr} \tag{10}$$

$$Q_s = \frac{V^2}{\omega_s L_s} V_s I_{qr} - \frac{L_m}{L_s} V_s I_{dr} \tag{11}$$

In order to keep the DC voltage constant regardless of the grid connections, the GSC (grid side converter) is used to regulate the DC terminal voltage of the back-to-back converters. In addition, a feed-forward control strategy is applied to control the active and reactive power quantities between the grid and the GSC [31]. This approach provides an effective solution for grid-compatible power management while ensuring that the DC link settings are maintained at a constant level.

The control system is designed as a system of synchronous reference frames (d-axis) aligned with the grid layout. This reference frame is considered as zero for the q-axis component (Vq) of the grid layout. The system has two main objectives. First, the DC link parameters provided by the current control I_d are kept at a predetermined fixed value. Second, the reactive power measurement I_q is controlled cyclically [31]. This strategy makes it possible to independently control both active power and reactive power and ensures that the system works in harmony with the grid. Correct modeling of wind turbine dynamics is a fundamental step in increasing the sustainability of variable energy production. Effectively optimizing these dynamics will constitute an important strategy to make energy production more efficient and to meet increasing energy consumption.

2.3 | Double-Fed Induction Generators

In DFIG, the stator winding is directly connected to the power grid. The rotor winding is made up of an inverter containing two mutual voltage sources using a four-quadrant power converter to connect to the grid. Generally, it is the job of the converter control system on the rotor side to regulate the electromagnetic torque and provide reactive power to maintain the magnetization of the machine. The job of regulating the direct current link belongs to the converter control system on the grid side [32]. A wind power system using a doubly fed asynchronous generator is shown in Figure 1.

DFIGs are frequently used in wind applications due to some of their superior features. DFIG has high efficiency and low installation cost compared to other generator topologies used in variable speed WECS due to the direct connection of the stator to the grid and the power electronic circuit in the rotor circuit, which can be selected at approximately 25% of the nominal stator power [16].

It is especially optimal for applications with high power requirements, as it has the capacity to produce energy beyond the nominal power. It can produce at specified power levels, from nominal speed to cut-off speed, in a wide speed range. DFIG plays a critical role in increasing efficiency throughout the system [15]. The transient performance of the doubly fed induction generator used in WECS has been investigated with the sixth order transfer function model given in Equation (12) and different search algorithms have been applied in the controller optimization of this model.

$$G(S) = \frac{0.000324s^6 - 1.75s^5 - 2366s^4 + 7.9 \times 10^6 s^3 + 7.5 \times 10^9 s^2 + 5 \times 10^{12} s + 2.18 \times 10^{14}}{s^6 + 2340s^5 + 8.67 \times 10^6 s^4 + 4.79 \times 10^9 s^3 + 2.7 \times 10^{12} s^2 + 1.27 \times 10^{14} s + 9.6 \times 10^{14}} \tag{12}$$

3 | The Hiking Optimizer

Metaheuristic algorithms are inspired by the functioning of natural systems to develop general approaches to optimization problems. HOA offers a new perspective on such algorithms and is inspired by the walking behaviors that people exhibit in their daily lives. The main goal of HOA is to reach the global optimum quickly and effectively.

17518652, 2025, 1, Downloaded from https://ietresearch.onlinelibrary.wiley.com/doi/10.1049/cth2.70071 by Bursa Uludag University Kutuphane ve Dokumantasyon, Wiley Online Library on [07/09/2026]. See the Terms and Conditions (https://onlinelibrary.wiley.com/terms-and-conditions) on Wiley Online Library for rules of use; OA articles are governed by the applicable Creative Commons License

HOA is based on the well-established Tobler's Walking Function, formulated by American-Swiss geographer and cartographer Waldo Tobler, as stated by Oladejo et al. [17]. This function provides an exponential model depending on the slope of the terrain that a hiker follows. Tobler's Walking Function estimates how fast hikers will walk on different slopes by incorporating terrain features. This model is known as an exponential function, especially used for hiking on terrain, and the distance over the slope of the trail is accurately reflected in the speed.

$$W_{i,t} = 6e^{-3.5\left|S_{i,t}+0.05\right|} \tag{13}$$

Here $W_{i,t}$ is the speed of the walker at time t and $S_{i,t}$ is the slope of the terrain. Also, the terrain slope $S_{i,t}$ is calculated as follows:

$$S_{i,t} = \frac{dh}{dx} = tan\theta_{i,\,t}. \tag{14}$$

Here, dh represents the vertical elevation change between two points, while dx defines the distance covered in the horizontal plane. However, $\theta_{i,t}$ i s considered as the slope angle of the terrain and this value varies between 0 and 50°. HOA leverages both the social dynamics of walkers as a group and the cognitive skills of individual walkers. A walker's current speed is calculated based on factors such as the lead walker's location, their current location, and the sweep factor (SF), in addition to the initial speed determined by Tobler's Gait Function (THF).

$$W_{i,t} = W_{i,t-1} + \gamma_{i,t}\ \left(\beta_{best} - \alpha_{i,t}\beta_{i,t}\right). \tag{15}$$

Here, $\gamma_{i,t}$ is defined as a random and uniformly distributed number in the range [0,1]. $W_{i,t}$ is the current speed of walker i, and $Wi_{,t-1}$ is the initial speed. βbest represents the position of the leader walker, while $\alpha_{i,t}$ is the SF defined in the range [1,3]. The SF acts as a control mechanism to prevent the walker from straying too far from the leader. This allows the walker to observe the leader's direction and perceive the signals given by the leader.

The new position of the walker reflects the effect of the current speed over time and expresses how the position changes. This is determined based on the walker's current position, the determined speed value, and the time step. In other words, $\beta_{i,t+1}$ is obtained by adding the speed value in Equation (13) to the walker's previous position. This formula is used to model the walker's displacement in the following steps.

$$\beta_{i,t+1} = \beta_{i,t} + W_{i,t} \tag{16}$$

The exploration and exploitation behaviours of HOA are driven by a parameter called the screening factor (SF). SF directly affects the distance between the trail leader and other hikers. At the same time, the trail slope, which determines the hiker speed defined in Equations (13) and (14), is also a critical element that shapes the exploration and exploitation tendencies of HOA. When the range of the SF parameter is widened, HOA focuses more on the exploitation phase.

On the other hand, narrowing the range of the SF range leads the system to exhibit more exploration behaviour. Similarly, narrowing the range of the slope angle of the trail causes HOA to exhibit more exploitation behaviour. Together, these parameters determine the behaviour and performance of HOA in optimization processes. The changes in factors such as SF and slope angle affect how the system establishes the balance between exploration and exploitation, thus shaping the solution generation strategies. Algorithm 1 explains the operation of the HOA step by step.

ALGORITHM 1 | Pseudocode of HOA.

Input: UB, LB, T, I, d

Prepare by predetermining the fitness vector RI × 1
F_{best} ← *Predetermine the best fitness vector* R(*T*+1) ×1
β ← *Initialize by randomly determining the positions of the hiker's* RI×*d*
for *i* ← *1 to I* ***do***
F_i ← *Measure the competence of the hiker's*
end for
$F_{best,\,1}$ ← *The best value of the walkers at the initial level*
for *t* ← *1 to T* ***do***
$F_{best,\,t}$ ← *Determine hiker with highest fitness*
β_{best} ← *Express the position of the best condition as* $F_{best,\,t}$
for *i* ← *1 to I* ***do***
    $\beta_{i,t}$ ← *Determine the initial position of hiker i*
    $\theta_{i,t}$ ← *Calculate the slope angle on the hiker's track*
    $S_{i,t}$ ← *Calculate the slope by (14)*
    $W_{i,t-1}$ ← *Calculate the initial hiking speed with (13)*
    $W_{i,t}$ ← *Determine the actual speed of hiker i using (15)*
    $\beta_{i,t+1}$ ← *Update the position of hiker i using (16)*
    $\beta_{i,t}$ ← *Determine the boundary* $\beta_{i,t+1}$ *within LB and U B*
    if $F_n \le F(n)$ ***then***
    $\gamma(n,\ :) \leftarrow \vec{H}$
    $F(n) \leftarrow F_n$
    end if
end for
$F_{sol}(i+1) \leftarrow min(F)$
end for
F_{sol} * ← *argmin* (F_{sol})
return

4 | Modified Objective Function Driven Hiking Optimizer Based PID Controlled DFIG System

PID controllers are among the most widely used control strategies in industrial applications due to their simplicity, versatility, and effectiveness [33]. A PID controller operates by continuously adjusting the control signal to minimize the error between a desired set point and the actual process variable. This feedback mechanism is critical for maintaining system stability, improving performance, and ensuring process efficiency in various industries, including manufacturing, energy, and chemical processing. The PID control strategy is based on three fundamental components of proportional (K_p), integral (K_i) and derivative (K_d).

17518652, 2025, 1, Downloaded from https://ietresearch.onlinelibrary.wiley.com/doi/10.1049/cth2.70071 by Bursa Uludag University Kutuphane ve Dokumantasyon, Wiley Online Library on [07/09/2026]. See the Terms and Conditions (https://onlinelibrary.wiley.com/terms-and-conditions) on Wiley Online Library for rules of use; OA articles are governed by the applicable Creative Commons License

The K_p component responds to the current error by applying a control signal proportional to the error. This component enhances system responsiveness but may lead to steady-state errors. The K_i component addresses accumulated past errors, eliminating steady-state deviations by integrating the error over time. Lastly, the K_d component anticipates future errors based on the rate of error change, adding a damping effect to minimize overshoot and oscillations. The standard PID controller equation is expressed as follows:

$$u\ (t) = K_p\, e\,(t) + K_i \int_0^t e\,(t)\, dt + K_d \frac{de\,(t)}{dt} \tag{17}$$

where $u(t)$ is the control signal, $e(t)$ is the error (set point—process variable) and K_p, K_i, K_d are proportional, integral, and derivative gains, respectively This equation reflects the combined effects of proportional, integral, and derivative actions, ensuring robust control for a wide range of applications. In advanced control systems, particularly in dynamic environments, such as DFIG systems, the standard PID controller may require fine-tuning to achieve optimal performance. Tuning the parameters (K_p, K_i, K_d) is critical to balancing competing objectives, such as minimizing overshoot, achieving fast settling times, and ensuring energy efficiency.

This study utilizes an enhanced version of the ZLG [34] cost function to optimize the tuning of standard PID controller parameters (K_p, K_i, K_d) for a DFIG system. The ZLG function, originally proposed for control system optimization, effectively balances transient and steady-state performance metrics [35]. The modifications introduced in this study extend the ZLG approach by incorporating additional penalty terms to address specific control challenges, such as overshoot, settling time, control effort, and the rate of change of control signals. The original ZLG objective function is formulated as:

$$ZLG = \left(1 - e^{-\beta}\right) \cdot \left(E_{ss} + \frac{OS}{100}\right) + e^{-\beta} \cdot (T_s - T_r) \tag{18}$$

where E_{ss} is steady-state error, approximated as the absolute difference between the minimum and maximum values of the settling region, OS is percentage overshoot, representing the maximum deviation from the setpoint, normalized by the setpoint value, T_s is settling time, the time required for the response to remain within 2% of the setpoint, T_r is rise time, the time required to reach 90% of the setpoint and β is a balancing factor that determines the relative weight of steady-state and transient performance. Larger values emphasize transient performance, while smaller values focus on steady-state accuracy. This original form of the ZLG function is designed to prioritize transient and steady-state performance, balancing fast responses and minimizing overshoot and steady-state error.

To improve the robustness and adaptability of the ZLG function for DFIG systems, this study introduces additional penalty terms that penalize undesirable control behaviours, such as excessive overshoot, prolonged settling times, high control efforts, and abrupt control signal changes. The proposed objective function is expressed as follows.

$$F = \frac{1}{2} \cdot \left(\left(1 - e^{-\beta}\right) \cdot \left(E_{ss} + \frac{OS}{100}\right) + e^{-\beta} \cdot (T_s - T_r) \right)$$
$$+ \frac{1}{2} \cdot \left(OS_{penality} + T_s{}^{penality} + CRP + CE \right) \tag{19}$$

In here, β denotes the balancing factor and was taken as 0.3, $OS_{penality}$ represents the overshoot penalty which is described as $OS_{penality} = OS^2$. This term penalizes large overshoot values to prevent system instability. The term $T_s{}^{penality}$ represents the settling time penalty discourages prolonged settling times, ensuring a faster response. The latter is described as $T_s{}^{penality} = T_s{}^2$. CRP denotes the control rate penalty and is described as follows.

$$CRP = \int_0^T \left(\frac{du\,(t)}{d\,(t)} \right)^2 dt \tag{20}$$

This term helps penalizing abrupt changes in the control signal, promoting smoother responses and reducing oscillations.

Lastly, CE stands for the control effort which penalizes excessive control action, ensuring energy-efficient operation. The latter term is formulated as follows.

$$CE = \int_0^T \left(\frac{1}{1+t} \right) .u(t)^2 dt \tag{21}$$

The inclusion of penalties for overshoot, settling time, control effort, and rate of change extends the original ZLG function to address practical challenges in control systems. Besides, the use of β dynamically adjusts the emphasis between steady-state and transient behaviors, ensuring a comprehensive optimization approach. By penalizing undesirable behaviours, the proposed function achieves smoother and more stable responses, particularly critical for DFIG systems under varying operational conditions. The enhanced ZLG function is better suited for DFIG systems, where stability, efficiency, and dynamic adaptability are essential. The HOA is used to adjust the ideal PID parameters via the proposed F objective function. Figure 2 demonstrates the process of the proposed method.

5 | Results

5.1 | Compared Algorithms

This study compares the performance of the HOA with five other metaheuristic algorithms including starfish optimization algorithm (SFOA) [20], GWO [21], DA [22], FDA [23], and SCA [24]. These algorithms were chosen based on their demonstrated efficiency in solving optimization problems and their recency in the literature, ensuring the evaluation incorporates state-of-the-art methodologies. For example, the SFOA is a bio-inspired algorithm that models the unique locomotion and regenerative capabilities of starfishes, making it particularly adept at adapting to complex and dynamic optimization landscapes. GWO, is a nature-inspired algorithm that simulates the hierarchical leadership and cooperative hunting strategies of grey wolves, emphasizing a balanced approach to exploration and exploitation. In a similar manner, the DA is inspired by the static and dynamic swarming behaviours of dragonflies and uses attraction and distraction forces to efficiently navigate the solution space. On the other hand, the FDA leverages principles from fluid dynamics to model the flow of solutions, optimizing paths based on flow direction efficiency. Unlike all of the above listed

17518652, 2025, 1, Downloaded from https://ietresearch.onlinelibrary.wiley.com/doi/10.1049/cth2.70071 by Bursa Uludag University Kutuphane ve Dokumantasyon, Wiley Online Library on [07/09/2026]. See the Terms and Conditions (https://onlinelibrary.wiley.com/terms-and-conditions) on Wiley Online Library for rules of use; OA articles are governed by the applicable Creative Commons License

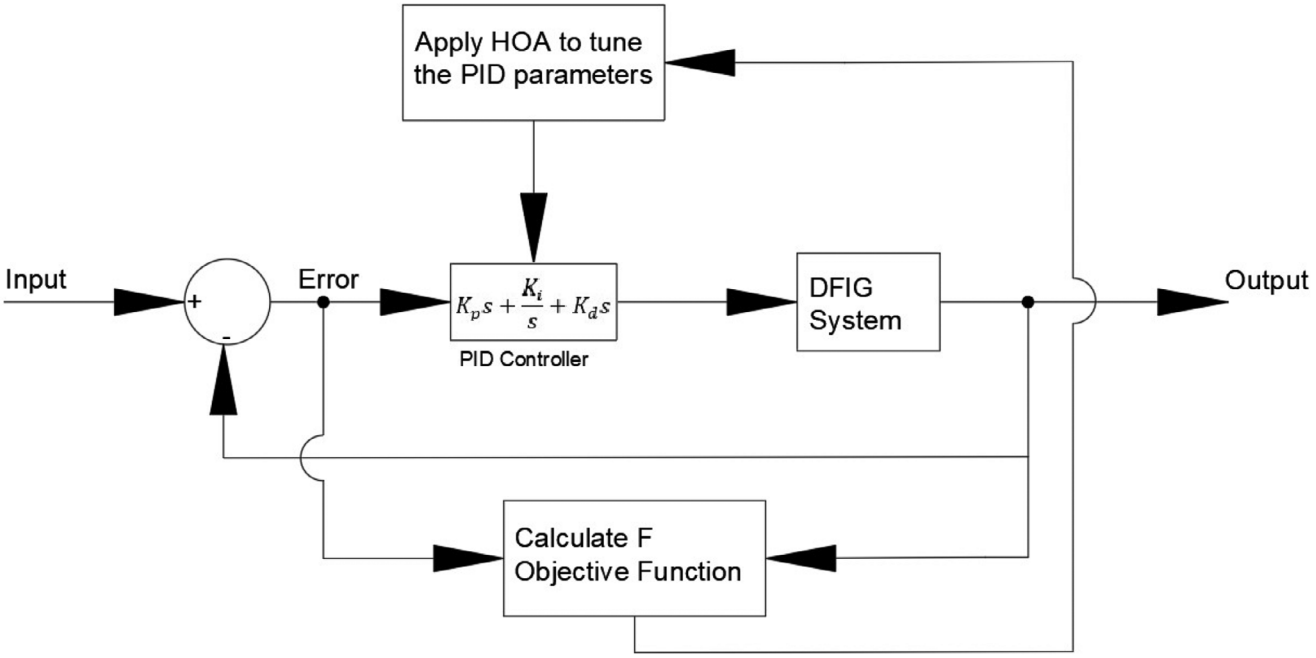


FIGURE 2 | Proposed HOA based PID controlled DFIG system.

algorithms used for the comparison, the SCA is a mathematically driven algorithm that employs sine and cosine functions to define dynamic search trajectories for global and local optimization.

For a fair and consistent evaluation, the default parameter values of each algorithm, as reported in their respective original publications, were utilized. This approach ensures that the performance assessment reflects the inherent strengths and design characteristics of the algorithms without bias from external parameter tuning. By comparing HOA with these selected algorithms under identical conditions, this study provides a robust framework for evaluating the relative effectiveness of various optimization strategies in the context of PID controller tuning for DFIG systems. To ensure reproducibility and technical clarity, the simulations were conducted using MATLAB Simulink R2025a on a personal computing environment powered by a 12th Gen Intel Core i7-1260P processor operating at 2.10 GHz and equipped with 16.0 GB of RAM. A fixed-step Runge-Kutta (ode4) solver was used with a sampling time of 0.001 s, which provides an effective trade-off between simulation accuracy and computational cost. The simulation time was set to 0.5 s, and the system responses were analysed using 1000 uniformly spaced time samples to capture both transient and steady-state behaviours with sufficient resolution.

5.2 | Statistical Results

The statistical performance metrics of the algorithms compared in this study provide a quantitative basis for evaluating the effectiveness and reliability of the HOA in tuning PID controllers. The metrics analysed include the best, worst, mean, median, and standard deviation of the objective function values achieved by each algorithm across 30 runs. Table 1 summarizes the obtained comparative results. As demonstrated, the HOA demonstrated the most consistent performance with a minimal standard deviation (0.0013) and a tightly clustered mean (0.1965) and median (0.196) values. These indicate high reliability and stability in the optimization process. On the other hand, the DA exhibited significant variability, with a large standard deviation (88.3058) and a wide gap between the best (0.21) and worst (441.8382) results. This suggests challenges in converging consistently to optimal solutions. The FDA achieved relatively better consistency than DA but still showed moderate variability. The best (0.2252) and worst (2.2742) values indicate some inconsistency in performance. The GWO delivered stable results with a standard deviation of 0.1085, although its best value (0.2016) was slightly less competitive compared to HOA. The SCA produced higher variability with a standard deviation of 0.1505, indicating less consistent convergence compared to HOA and GWO. Lastly, the SFOA performed closely to HOA, with a standard deviation of 0.0036 and a best value (0.1973) near HOA's best (0.1952), but with slightly less precision. The results indicate that HOA outperforms the other algorithms in terms of consistency and precision, which are critical for robust PID controller tuning. The low standard deviation highlights HOA's ability to reliably converge to optimal solutions, while the narrow range of its best

TABLE 1 | The statistical metrics obtained from compared algorithms.

Algorithm	Best	Worst	Mean	Median	Standard deviation
HOA	0.1952	0.2002	0.1965	0.196	0.0013
DA	0.2100	441.8382	17.9704	0.2963	88.3058
FDA	0.2252	2.2742	0.3788	0.2898	0.4014
GWO	0.2016	0.6230	0.3212	0.2897	0.1085
SCA	0.2212	0.6846	0.3649	0.2882	0.1505
SFOA	0.1973	0.2110	0.2098	0.1959	0.0036

17518652, 2025, 1, Downloaded from https://ietresearch.onlinelibrary.wiley.com/doi/10.1049/cth2.70071 by Bursa Uludag University Kutuphane ve Dokumantasyon, Wiley Online Library on [07/09/2026]. See the Terms and Conditions (https://onlinelibrary.wiley.com/terms-and-conditions) on Wiley Online Library for rules of use; OA articles are governed by the applicable Creative Commons License

TABLE 2 | Wilcoxon's signed rank test.

Comparison	*p*-value	Significance
HOA vs. SCA	1.86×10^{-9}	Yes
HOA vs. SFOA	3.86×10^{-7}	Yes
HOA vs. DA	4.65×10^{-8}	Yes
HOA vs. FDA	1.86×10^{-9}	Yes
HOA vs. GWO	1.55×10^{-2}	Yes

and worst values underscores its effectiveness in maintaining performance across multiple trials. This statistical analysis supports the superior capability of HOA in addressing the challenges of PID controller parameter optimization for DFIG systems under dynamic conditions.

To validate the observed performance differences statistically, the Wilcoxon signed-rank test [36] was conducted between the HOA-based controller and five competing optimization algorithms. As reported in Table 2, all pairwise comparisons resulted in p-values below the conventional 0.05 threshold, confirming statistically significant differences. Notably, HOA outperformed SCA, SFOA, DA, and FDA with highly significant margins ($p < 10^{-7}$). Although the margin against GWO was comparatively narrower ($p = 1.55 \times 10^{-2}$), it still meets the criterion for statistical significance. These results confirm that the superior performance of the HOA-based PID tuning approach is not only evident in average performance metrics but also statistically reliable across multiple runs.

5.3 | Convergence Curves and Obtained Parameters for the Standard PID Controller

The convergence behaviour of the HOA and the five comparative algorithms (DA, FDA, GWO, SCA, and SFOA) is analysed in this section. The study evaluates the ability of each algorithm to optimize the PID controller parameters (K_p, K_i, K_d) for the DFIG system. Figure 3 depicts the convergence curves of all algorithms, showing the progression of the objective function value with iteration count. From the curves, the HOA demonstrates rapid convergence toward the optimal solution, achieving stability within a minimal number of iterations. This indicates its efficiency in balancing exploration and exploitation phases during optimization. GWO and SFOA exhibit competitive convergence behaviour, approaching optimal solutions relatively quickly but requiring more iterations compared to HOA to stabilize. DA, FDA and SCA display slower convergence rates, reflecting challenges in efficiently navigating the search space and fine-tuning parameters.

Table 3 presents the optimized PID parameters (K_p, K_i, K_d) obtained by each algorithm. HOA achieved parameters that reflect its superior ability to minimize the objective function and meet the performance criteria. The HOA yielded parameter values that align with the objective of minimizing overshoot, settling time, and control effort while ensuring system stability. Its ability to achieve a fine-tuned balance between these competing objectives is evident. GWO and SFOA performed closely, achieving competitive parameter values, though slightly less optimal compared to HOA. DA, FDA, and SCA demonstrated suboptimal parameter tuning, with higher proportional and integral gains leading to less stable control behavior. The results from convergence curves and obtained parameters substantiate HOA's effectiveness and reliability in optimizing PID controllers for complex systems like DFIG under varying operational conditions. This capability underscores its potential as a robust tool for industrial control applications.

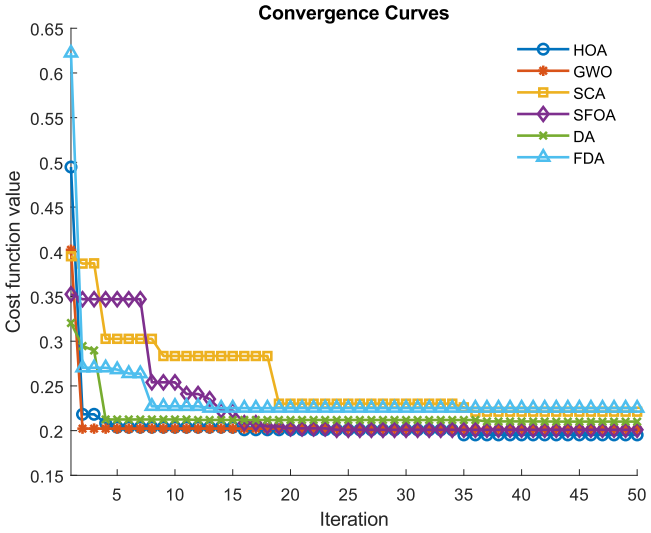


FIGURE 3 | Comparative convergence curves with respect to iteration numbers.

TABLE 3 | The obtained parameters of the standard PID controller via HOA, DA, FDA, GWO, SCA, and SFOA.

Algorithm	K_p	K_i	K_d
HOA	19.5881	176.288	0.0064
DA	15.1118	133.4676	0.1093
FDA	13.4197	123.8447	0.0651
GWO	20	186.2713	0.0012
SCA	14.8677	138.9476	0.0042
SFOA	20	185.7454	0.001

5.4 | Time Response Analysis

The time-domain response of the PID controller optimized by the HOA and five comparative algorithms (DA, FDA, GWO, SCA, and SFOA) is analysed in this section. The analysis includes key performance metrics such as overshoot, rise time, settling time, and peak time. Figures 4 and 5 provide visual representations of the comparative step response profiles and steady-state error values, respectively, while the numerical results are summarized in Table 4.

As can be observed from the provided analyses, the HOA exhibited zero overshoot, indicating excellent stability and precise control, making it the most reliable algorithm for DFIG systems

17518652, 2025, 1, Downloaded from https://ietresearch.onlinelibrary.wiley.com/doi/10.1049/cth2.70071 by Bursa Uludag University Kutuphane ve Dokumantasyon, Wiley Online Library on [07/09/2026]. See the Terms and Conditions (https://onlinelibrary.wiley.com/terms-and-conditions) on Wiley Online Library for rules of use; OA articles are governed by the applicable Creative Commons License

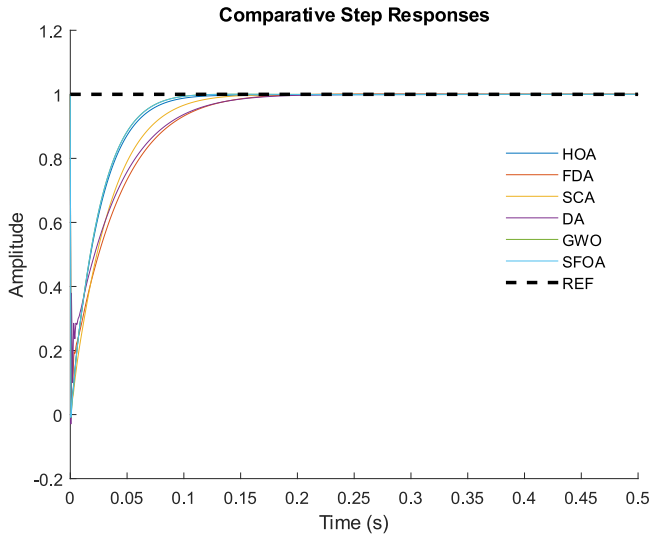


FIGURE 4 | Comparative step responses for HOA, FDA, SCA, DA, GWO, and SFOA.

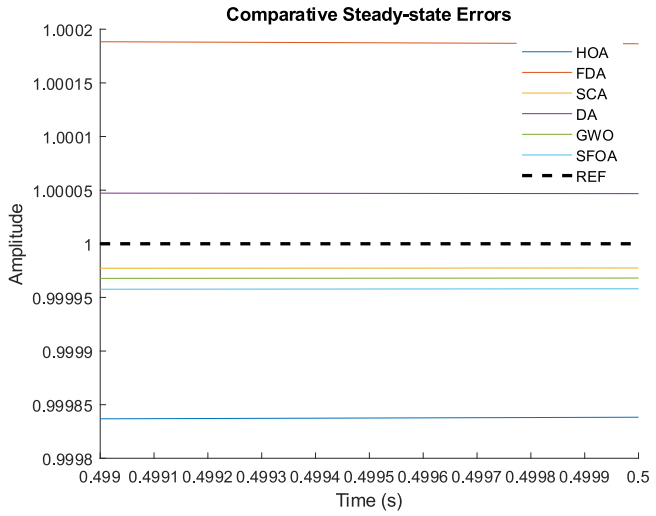


FIGURE 5 | Comparative steady-state error values obtained from application of HOA, FDA, SCA, DA, GWO, and SFOA.

with high-performance requirements. FDA and SFOA showed minor overshoots (0.96425 % and 0.0056227 %, respectively), while GWO exhibited a slightly higher overshoot (0.039555%). In terms of rise time, all algorithms achieved zero rise times, demonstrating fast responsiveness to step changes. For the settling time, the HOA achieved a short settling time of 0.08922 s, highlighting its ability to quickly stabilize the system. Other algorithms, such as FDA and DA, had longer settling times of 0.1397 and 0.13994 s, respectively, while GWO performed slightly better with a settling time of 0.082414 s. For the peak time, HOA achieved zero peak time, further reinforcing its superior damping and stability performance. Other algorithms, such as FDA and SFOA, showed small peak times (0.24728 s and 0.13749 s, respectively).

Figure 5 illustrates the steady-state error values for all compared algorithms. All methods exhibited steady-state errors that were very close to the reference line. The HOA, FDA, SCA, DA, GWO, and SFOA converged near the reference line, indicating small errors. The HOA effectively achieved near-zero values, demonstrating a negligible steady-state error similar to other approaches. This reinforces HOA's capability to maintain control precision in steady-state conditions, which is critical for ensuring reliability in industrial applications.

TABLE 4 | The numerical values for the time response metrics obtained for HOA, FDA, SCA, DA, GWO, and SFOA.

Algorithm	Overshoot	Rise time	Settling time	Peak time
HOA	0	0	0.08922	0
FDA	0.96425	0	0.1397	0.24728
SCA	0	0	0.11321	0
DA	0	0	0.13994	0
GWO	0.039555	0	0.082414	0.14557
SFOA	0.0056227	0	0.08269	0.13749

Table 4 presents the time response metrics for all algorithms. It is worth noting that a rise time of zero indicates that the system response, under ideal PID control, reached the 10%–90% transition threshold within a single simulation time step. This behavior reflects the steep dynamic response of the ideal controller in a noise-free simulation environment and is consistent with the rapid rise observed in Figure 4. The remaining results demonstrate that HOA outperforms the other algorithms in key time-response metrics, particularly in minimizing overshoot and settling time. This superior performance highlights HOA's capability to ensure fast and stable responses, which are critical for the dynamic and sensitive nature of DFIG systems.

5.5 | Frequency Response Analysis

The frequency response of the PID controllers optimized using the HOA and the comparative algorithms (DA, FDA, GWO, SCA, and SFOA) is analysed in this section. Frequency response analysis is critical for evaluating the stability, robustness, and dynamic performance of control systems under varying conditions. Figure 6 illustrates the Bode plots for all compared algorithms. As can be observed from the figure, the HOA achieved the highest phase margin of 87.163 degrees, indicating superior stability and robustness to phase disturbances. Other algorithms exhibited lower phase margins, with FDA and DA showing comparatively reduced stability. The HOA also demonstrated a gain margin of 26.11 dB, highlighting its ability to maintain stability under varying gain conditions. SFOA and GWO also exhibited competitive gain margins; however, slightly lower than HOA. The frequency response analysis clearly indicates that HOA outperforms the other algorithms in terms of phase and gain margins. These results are indicative of a robust PID controller design capable of handling dynamic and uncertain conditions in DFIG systems. The frequency response analysis reinforces the superiority of HOA in optimizing PID controllers, particularly in terms of stability and robustness. This performance makes HOA the most reliable choice for managing the challenging dynamics of DFIG systems in industrial applications.

17518652, 2025, 1, Downloaded from https://ietresearch.onlinelibrary.wiley.com/doi/10.1049/cth2.70071 by Bursa Uludag University Kutuphane ve Dokumantasyon, Wiley Online Library on [07/09/2026]. See the Terms and Conditions (https://onlinelibrary.wiley.com/terms-and-conditions) on Wiley Online Library for rules of use; OA articles are governed by the applicable Creative Commons License

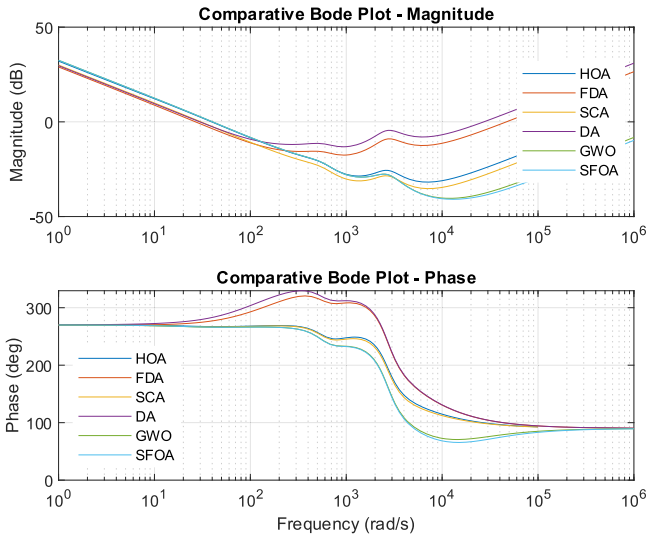


FIGURE 6 | Comparative Bode plots obtained for HOA, FDA, SCA, DA, GWO and SFOA.

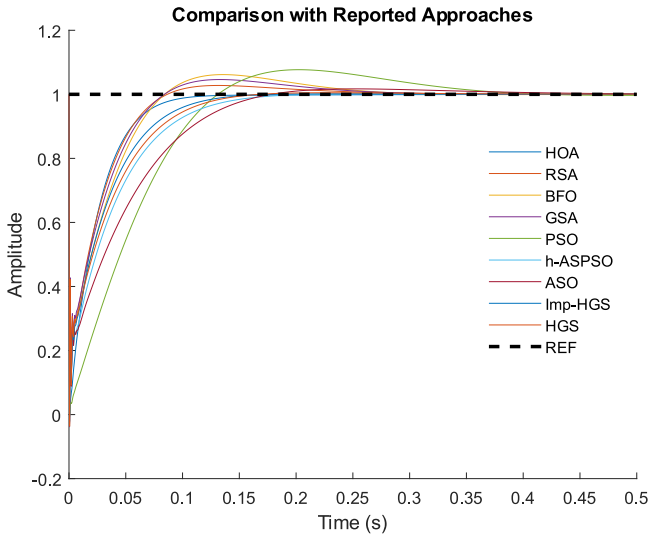


FIGURE 7 | Comparative step responses for HOA, RSA, BFO, GSA, PSO, h-ASO, ASO, Imp-HGS, and HGS.

TABLE 5 | The reported parameter values the standard PID controller via RSA, BFO, GSA, PSO, h-ASO, ASO, Imp-HGS and HGS.

Algorithm (%)	K_p	K_i	K_d
RSA	18.7151	227.6068	0.08735
BFO	14.9400	240.4000	0.1189
GSA	16.9400	242.4000	0.1191
PSO	6.2392	111.4924	0.0099
h-ASPSO	13.6145	124.9119	0.08982
ASO	10.0207	109.2884	0.1122
Imp-HGS	16.4211	150.5726	0.09552
HGS	14.9782	142.4485	0.1183

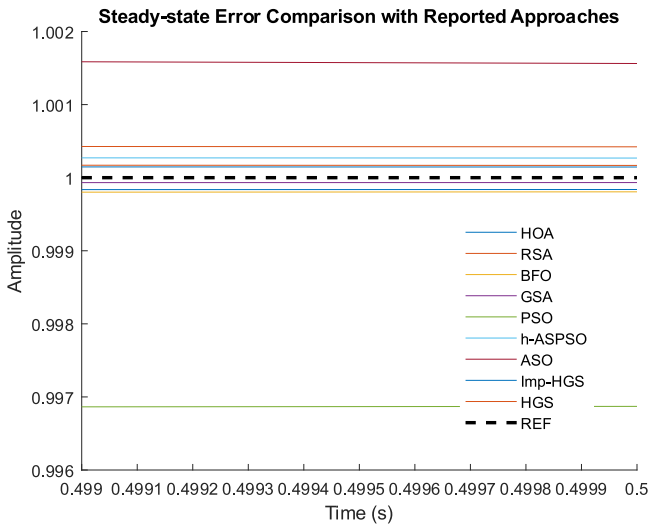


FIGURE 8 | Comparative steady-state error values obtained from application of HOA, RSA, BFO, GSA, PSO, h-ASO, ASO, Imp-HGS, and HGS.

5.6 | Comparison With Reported Literature

To further evaluate the performance of the HOA, a comparison was conducted with reported optimization methods from existing literature. These methods include the RSA [25], BFO [26], GSA [26], PSO [26], ASO, and hybrid atom search (h-ASPSO) [27], hunger games search (HGS) algorithm and its improved version (Imp-HGS) [28]. Table 5 highlights the optimized PID parameters (K_p, K_i, K_d) obtained by the reported approaches.

Figure 7 visually compares the step responses of HOA with other algorithms. HOA's response is characterized by minimal overshoot, rapid stabilization, and smooth dynamics, outperforming all competitors. The step responses of methods like RSA, BFO, and PSO exhibit notable overshoots and longer stabilization times. Figure 8 highlights the steady-state errors across algorithms. HOA achieves a negligible error, maintaining control precision superior to others. Algorithms such as BFO, GSA, and PSO display significantly higher steady-state errors, indicating less precise control. HOA surpasses the reported optimization methods in both parameter optimization and time response performance. Figures 7 and 8 substantiate HOA's superiority, showcasing its robust design, superior dynamic performance, and precision in steady-state control. These results affirm HOA's suitability as an advanced optimization technique for PID controller design in high-performance applications.

Table 6 presents the time response characteristics of each algorithm, including overshoot, rise time, settling time, and peak time. HOA outperformed all other methods by achieving zero overshoot, the shortest settling time, and no peak time. HOA achieved a zero overshoot, ensuring system stability without excessive output deviation. It also provided the fastest settling time (0.08922 s), minimizing the time required for the system to stabilize. Besides, it demonstrated the least steady-state error, confirming its effectiveness in maintaining precise control over time.

17518652, 2025, 1, Downloaded from https://ietresearch.onlinelibrary.wiley.com/doi/10.1049/cth2.70071 by Bursa Uludag University Kutuphane ve Dokumantasyon, Wiley Online Library on [07/09/2026]. See the Terms and Conditions (https://onlinelibrary.wiley.com/terms-and-conditions) on Wiley Online Library for rules of use; OA articles are governed by the applicable Creative Commons License

TABLE 6 | The numerical values for the time response metrics obtained for HOA, RSA, BFO, GSA, PSO, h-ASO, ASO, Imp-HGS, and HGS.

Algorithm	Overshoot	Rise time	Settling time	Peak time
HOA	0	0	0.08922	0
RSA	2.7713	0	0.17919	0.13171
BFO	6.1632	0	0.2309	0.13554
GSA	4.6206	0	0.216	0.13296
PSO	7.6927	0	0.33503	0.20242
h-ASPO	0.028525	0	0.1429	0.21839
ASO	1.7031	0	0.15389	0.25134
Imp-HGS	0.14572	0	0.11912	0.21656
HGS	0.37179	0	0.12725	0.19273

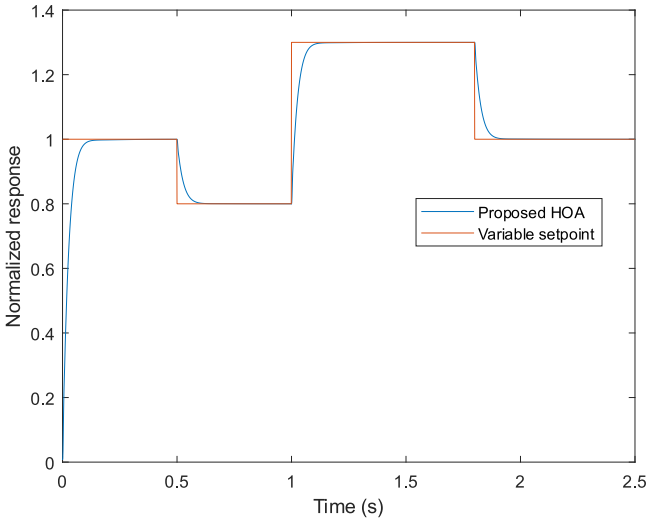


FIGURE 9 | Tracking performance of the HOA based approach for variable input.

5.7 | Input Signal Tacking Performance

The input signal tracking performance of the PID controller optimized by the HOA was evaluated to determine its capability to accurately follow varying reference signals. Figure 9 illustrates the tracking performance of HOA for a variable input signal to test dynamic responsiveness. HOA demonstrated exceptional tracking accuracy, with the output closely following the input signals under both steady-state and dynamic conditions. This highlights the precise control achieved by HOA-optimized PID parameters. During sudden changes in input (step response), the system showed minimal overshoot and a rapid stabilization time. These characteristics ensure the system's reliability during abrupt input variations, critical for dynamic environments like wind energy systems. HOA exhibited consistent performance, maintaining stability and accuracy even under challenging dynamic scenarios. This robustness underscores the adaptability of HOA-optimized controllers for complex industrial systems. The superior tracking performance demonstrated by HOA reflects its potential

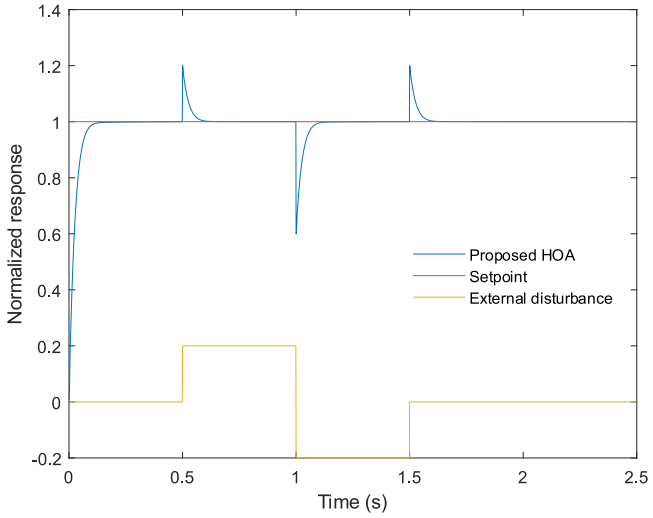


FIGURE 10 | Performance of the HOA based approach for the external disturbance rejection ability.

in industrial applications, particularly for systems like DFIG where precise control over fluctuating inputs is critical. This performance further validates HOA's suitability as a robust optimization approach for PID controller design.

5.8 | External Disturbance Rejection Ability

The ability of the PID controller optimized using the HOA to reject external disturbances was evaluated under dynamic operating conditions. This evaluation is crucial for determining the robustness and reliability of the controller in real-world industrial applications, such as in DFIG systems, where external disturbances are inevitable. Figure 10 illustrates the performance of the HOA-based controller in rejecting disturbances applied to the system. HOA-optimized PID controllers demonstrated remarkable resilience to external disturbances. When disturbances were applied, the system rapidly mitigated their impact, restoring the output to the desired set point with minimal deviation. The system exhibited negligible overshoot during disturbance rejection, ensuring stable operation without instability. Furthermore, the settling time was significantly short, reflecting the controller's efficiency in counteracting external perturbations. HOA maintained robust performance across varying disturbance magnitudes and durations, emphasizing its adaptability to dynamic changes. This capability is critical for ensuring uninterrupted operation in industrial applications. The external disturbance rejection analysis validates the robustness and reliability of the HOA-optimized PID controller. Its superior performance under varying disturbance conditions ensures that it is well-suited for demanding industrial environments where external perturbations are a regular challenge. These results further emphasize the efficacy of HOA as a robust optimization technique for PID control design.

6 | Conclusion and Recommendation for Future Works

This study presented a novel approach to optimizing PID controller parameters for DFIG systems, leveraging the HOA coupled

17518652, 2025, 1, Downloaded from https://ietresearch.onlinelibrary.wiley.com/doi/10.1049/cth2.70071 by Bursa Uludag University Kutuphane ve Dokumantasyon, Wiley Online Library on [07/09/2026]. See the Terms and Conditions (https://onlinelibrary.wiley.com/terms-and-conditions) on Wiley Online Library for rules of use; OA articles are governed by the applicable Creative Commons License

with an enhanced ZLG objective function. The proposed method effectively addresses critical challenges in control systems, such as minimizing overshoot, reducing settling time, maintaining steady-state precision, and enhancing robustness against external disturbances. Comparative evaluations against five state-of-the-art algorithms and benchmarks from existing literature demonstrated the superiority of HOA in achieving optimal transient and steady-state performance metrics. The HOA-based PID controller showcased remarkable capabilities, including zero overshoot, rapid stabilization, and excellent disturbance rejection. The method's adaptability to varying operating conditions and input profiles underscores its potential for practical applications in dynamic industrial environments. This work advances the state-of-the-art in PID controller optimization, making significant contributions to renewable energy systems and other industries reliant on robust control strategies.

Building on the promising results of this study, several avenues for future research are identified. The first one is related to exploration of the application of HOA for multi-objective optimization problems, such as balancing economic efficiency, environmental impact, and control precision in renewable energy systems. The second one concerns the investigation of the performance of HOA in optimizing controllers for nonlinear, time-varying systems, broadening its applicability to complex, real-world scenarios. A third direction involves combining HOA with adaptive or model-predictive control strategies to enhance real-time performance and adaptability in dynamically changing environments. In addition, while this study focused on fixed and deterministic disturbance profiles, real-world wind energy systems often experience inherently stochastic wind speed variations. These fluctuations can significantly influence the control performance and dynamic response of WECS. Therefore, future work could integrate stochastic wind models or turbulence-based input profiles to evaluate the resilience and adaptability of the proposed HOA-based PID controller under more realistic environmental conditions. More avenues can also be investigated such as testing the scalability and computational efficiency of HOA in optimizing controllers for large-scale systems, such as multi-area power grids or hybrid renewable energy systems, assessing the resilience of HOA-optimized controllers under noisy measurement conditions and model uncertainties to validate their robustness in practical deployments, and extending the application of HOA to other domains, such as robotics, process control, and autonomous systems, to evaluate its versatility in diverse optimization challenges.

Author Contributions

Davut Izci: conceptualization, methodology, software, visualization, investigation, writing – original draft preparation. **Fatma Artun:** conceptualization, methodology, software, visualization, investigation, writing – original draft preparation. **Serdar Ekinci:** data curation, validation, supervision, resources, writing – review and editing. **Mohit Bajaj:** project administration, supervision, resources, writing – review and editing. **Ievgen Zaitsev:** project administration, supervision, resources, writing – review and editing. **Vojtech Blazek:** project administration, supervision, resources, writing – review and editing.

Acknowledgements

This research is funded by European Union under the REFRESH—Research Excellence For Region Sustainability and High-Tech Industries Project via the Operational Programme Just Transition under Grant CZ.10.03.01/00/22_003/0000048; in part by the National Centre for Energy II and ExPEDite Project a Research and Innovation Action to Support the Implementation of the Climate Neutral and Smart Cities Mission Project TN02000025; and in part by ExPEDite through European Union's Horizon Mission Programme under Grant 101139527. The authors would like to express their sincere gratitude to Lukas Prokop and Stanislav Misak for their exceptional supervision, project administration, and overall guidance throughout the course of this project. Their expertise and support were instrumental to its success.

Conflicts of Interest

The authors declare no conflicts of interest.

Data Availability Statement

The datasets used and/or analysed during the current study available from the corresponding author on reasonable request.

References

1. M. Jabari, D. Izci, S. Ekinci, M. Bajaj, V. Blazek, and L. Prokop, "A Novel Artificial Intelligence Based Multistage Controller for Load Frequency Control in Power Systems," *Scientific Reports* 14, no. 1 (2024): 29571.

2. S. Ekinci, R. M. Rizk-Allah, D. Izci, and E. Çelik, "Multi-Strategy Improved Runge Kutta Optimizer and Its Promise to Estimate the Model Parameters of Solar Photovoltaic Modules," *Heliyon* 10, no. 20 (2024): e39301.

3. B. Kumar., K. S. Sandhu, and R. Sharma, "Comparative Analysis of Control Schemes for DFIG-Based Wind Energy System," *Journal of The Institution of Engineers (India): Series B* 103, no. 2 (2022): 649–668.

4. M. Anju, K. V. Shihabudheen, and S. J. Mija, "Enhancing Grid Stability: A Hybrid Control Strategy for DFIG-Based Wind Turbines to Mitigate Sub-Synchronous Oscillations," *Electrical Engineering* 107 (2025): 8613–8644.

5. A. S. Veerendra, M. Vasavi Uma maheswari, K. Peddakapu, and C.h. Punya sekhar, "Enhancement of a Grid-Connected DFIG Wind Turbine System Using Fractional Order PI Controllers," *Renewable Energy Focus* 47 (2023): 100506.

6. M.d.S. Arifin, M. N. Uddin, and W. Wang, "Neuro-Fuzzy Adaptive Direct Torque and Flux Control of a Grid-Connected DFIG-WECS With Improved Dynamic Performance," *IEEE Transactions on Industry Applications* 59, no. 6 (2023): 7692–7700.

7. M. H. Suid and M. A. Ahmad, "Optimal Tuning of Sigmoid PID Controller Using Nonlinear Sine Cosine Algorithm for the Automatic Voltage Regulator System," *Isa Transactions* 128 (2022): 265–286.

8. L. Li, "A Novel Optimization Control of Gas Turbine Based on a Hybrid Method Using the BELBIC and Adaptive Multi Input Multi Output Feedback Control," *Journal of Intelligent & Fuzzy Systems* 45, no. 1 (2023): 863–876.

9. X. Hu, W. Tan, and G. Hou, "PIDD2 Control of Large Wind Turbines Pitch Angle," *Energies* 16, no. 13 (2023): 5096.

10. A. H. Yakout, W. Sabry, A. Y. Abdelaziz, H. M. Hasanien, K. M. AboRas, and H. Kotb, "Enhancement of Frequency Stability of Power Systems Integrated With Wind Energy Using Marine Predator Algorithm Based PIDA Controlled STATCOM," *Alexandria Engineering Journal* 61, no. 8 (2022): 5851–5867.

11. Y. A. Ali and M. Ouassaid, "Towards Alleviating Operating Conditions of MPC Controlled VSC for DFIG-Based Wind Turbines Using PSO Algorithm," in *2024 6th Global Power, Energy and Communication Conference (GPECOM)* (2024): 487–493.

17518652, 2025, 1, Downloaded from https://ietresearch.onlinelibrary.wiley.com/doi/10.1049/cth2.70071 by Bursa Uludag University Kutuphane ve Dokumantasyon, Wiley Online Library on [07/09/2026]. See the Terms and Conditions (https://onlinelibrary.wiley.com/terms-and-conditions) on Wiley Online Library for rules of use; OA articles are governed by the applicable Creative Commons License

12. A. Milles, A. Belhait, S. Ghoudelbourk, et al., "Optimizing PI Regulators for DFIGs in Wind Energy Using Artificial Intelligence," in *2024 2nd International Conference on Electrical Engineering and Automatic Control (ICEEAC)* (2024): 1–6.

13. Y. Sahri, S. Tamalouzt, S. Lalouni Belaid, et al., "Advanced Fuzzy 12 DTC Control of Doubly Fed Induction Generator for Optimal Power Extraction in Wind Turbine System Under Random Wind Conditions," *Sustainability* 13, no. 21 (2021): 11593.

14. R. K. Kumarb and J. Choudhary, "Design of a Novel Control Scheme for the Operation of the Doubly Fed Induction Generator," *Archives of Electrical Engineering* (2024): 373–392.

15. A. Sabo, T. Ebuka Odoh, V. Veerasamy, and N. I. Abdul Wahab, "Modified Multimachine Power System Design With DFIG-WECS and Damping Controller," *Energies* 17, no. 8 (2024): 1841.

16. S. Prakash and S. Radheswari, "Improved DFIG-Based Power Quality Controller Based on Machine Learning Cascaded Neural Networks," in *2023 International Conference on Energy, Materials and Communication Engineering (ICEMCE)* (2023): 1–6.

17. S. O. Oladejo, S. O. Ekwe, and S. Mirjalili, "The Hiking Optimization Algorithm: A Novel human-Based Metaheuristic Approach," *Knowledge-Based Systems* 296 (2024): 111880.

18. M. F. Goodchild, "Beyond Tobler's Hiking Function," *Geographical Analysis* 52, no. 4 (2020): 558–569.

19. D. Izci, "Design and Application of an Optimally Tuned PID Controller for DC Motor Speed Regulation via a Novel Hybrid Lévy Flight Distribution and Nelder–Mead Algorithm," *Transactions of the Institute of Measurement and Control* 43, no. 14 (2021): 3195–3211.

20. C. Zhong, G. Li, Z. Meng, H. Li, A. R. Yildiz, and S. Mirjalili, "Starfish Optimization Algorithm (SFOA): A Bio-Inspired Metaheuristic Algorithm for Global Optimization Compared With 100 Optimizers," *Neural Computing and Applications* 37 (2025): 3641–3683.

21. S. Mirjalili, S. M. Mirjalili, and A. Lewis, "Grey Wolf Optimizer," *Advances in Engineering Software* 69 (2014): 46–61.

22. S. Mirjalili, "Dragonfly Algorithm: A New Meta-Heuristic Optimization Technique for Solving Single-Objective, Discrete, and Multi-Objective Problems," *Neural Computing and Applications* 27, no. 4 (2016): 1053–1073.

23. B. S. Yildiz, N. Pholdee, P. Mehta, et al., "A Novel Hybrid Flow Direction Optimizer-DEynamic Oppositional Based Learning Algorithm for Solving Complex Constrained Mechanical Design Problems," *Materials Testing* 65, no. 1 (2023): 134–143.

24. L. Abualigah and A. Diabat, "Advances in Sine Cosine Algorithm: A Comprehensive Survey," *Artificial Intelligence Review* 54, no. 4 (2021): 2567–2608.

25. D. Izci, S. Ekinci, C. Budak, and V. Gider, "PID Controller Design for DFIG-Based Wind Turbine via Reptile Search Algorithm," in *2022 Global Energy Conference (GEC)* (2022): 154–158.

26. O. P. Bharti, K. Sarita, A. S. S. Vardhan, A. S. S. Vardhan, and R. K. Saket, "Controller Design for DFIG-based WT Using Gravitational Search Algorithm for Wind Power Generation," *IET Renewable Power Generation* 15, no. 9 (2021): 1956–1967.

27. D. Izci, S. Ekinci, and A. G. Hussien, "Effective PID Controller Design Using a Novel Hybrid Algorithm for High Order Systems," *PLoS ONE* 18, no. 5 (2023): e0286060.

28. S. Ekinci, D. Izci, E. Eker, L. Abualigah, C.-L. Thanh, and S. Khatir, "Hunger Games Pattern Search With Elite Opposite-Based Solution for Solving Complex Engineering Design Problems," *Evolving Systems* 15, no. 3 (2024): 939–964.

29. P. M. Anderson and A. A. Fouad, "Power System Control and Stability," (2002).

30. S. Müller, M. Deicke, and R. W. de Doncker, "Doubly Fed Induction Generator Systems for Wind Turbines: A Viable Alternative to Adjust Speed Over a Wide Range at Minimal Cost," *IEEE Industry Applications Magazine* 8, no. 3 (2002): 26–33.

31. J. Morren and S. W. H. deHaan, "Ridethrough of Wind Turbines With Doubly-Fed Induction Generator During a Voltage Dip," *IEEE Transactions on Energy Conversion* 20, no. 2 (2005): 435–441.

32. A. Loulijat, H. Chojaa, M. El Marghichi, et al., "Application and Comparison of a Modified Protection Scheme Utilizing a Proportional–Integral Controller With a Conventional Design to Enhance Doubly Fed Induction Generator Wind Farm Operations During a Balanced Voltage Dip," *Processes* 11, no. 10 (2023): 2834.

33. E. Eker, S. Ekinci, and D. İzci, "Optimal PID Controller Design for Liquid Level Tank via Modified Artificial Hummingbird Algorithm," Computer Science (2023): IDAP-2023, 37–43.

34. Ö. Can, C. Andiç, S. Ekinci, and D. Izci, "Enhancing Transient Response Performance of Automatic Voltage Regulator System by Using a Novel Control Design Strategy," *Electrical Engineering* 105, no. 4 (2023): 1993–2005.

35. S. Ekinci, D. Izci, and M. Yilmaz, "Efficient Speed Control for DC Motors Using Novel Gazelle Simplex Optimizer," *IEEE Access* 11 (2023): 105830–105842.

36. D. Izci, S. Ekinci, and B. Hekimoğlu, "A Novel Modified Lévy Flight Distribution Algorithm to Tune Proportional, Integral, Derivative and Acceleration Controller on Buck Converter System," *Transactions of the Institute of Measurement and Control* 44, no. 2 (2022): 393–409.

17518652, 2025, 1, Downloaded from https://ietresearch.onlinelibrary.wiley.com/doi/10.1049/cit2.70071 by Bursa Uludag University Kutuphane ve Dokumantasyon, Wiley Online Library on [07/09/2026]. See the Terms and Conditions (https://onlinelibrary.wiley.com/terms-and-conditions) on Wiley Online Library for rules of use; OA articles are governed by the applicable Creative Commons License